DOI: 10.1002/ ((please add manuscript number))
Article type: Full Paper

Interactions Between an Aryl Thioacetate-Functionalized Zn(II) Porphyrin and Graphene Oxide

*Boyang Mao[a], David G. Calatayud[a], Vincenzo Mirabello[a], Benjamin J. Hodges[a], José Alberto Ribeiro Martins[b], Stanley W. Botchway[c], John M. Mitchels[a] and Sofia I. Pascu[a]**

Dr. B. Mao, Dr. D. G. Calatayud, Dr. V. Mirabello, Dr. J. Mitchels, Dr. S. I. Pascu
Department of Chemistry, University of Bath, Claverton Down, BA2 7AY, Bath, UK
E-mail: s.pascu@bath.ac.uk
Dr. J. A. Martins
Centro de Engenharia Biológica and Departamento de Química, Universidade do Minho, Campus de Gualtar, 4710-057 Braga, Portugal
Prof. S. W. Botchway
Central Laser Facility, Rutherford Appleton Laboratory, Research Complex at Harwell, STFC Didcot OX11 0QX, UK

Keywords: porphyrin, graphene oxide, AFM studies, UV-vis titrations, fluorescence emission titrations

The surface modification of graphene oxide is carried out via a supramolecular functionalization using a Zn(II)-porphyrin soluble in common organic solvents on basis of long alkyl chains present at the exocyclic positions. This acts as dispersing agent and decorates the surface of the graphene oxide uniformly, giving rise to a new nanohybrid denoted Zn(II)-porphyrin@GO. The resulting Zn(II)-porphyrin@GO nanohybrid forms a stable dispersion in ethanol (was characterized by various spectroscopic techniques such as UV-vis, FT-IR, Raman). The morphology of Zn(II)-porphyrin@GO nanohybrid is investigated by AFM and TEM /SAED. Both TEM and AFM measurements indicate that the Zn(II)-porphyrin self-assemble onto the surface of graphene oxide sheets. Steady-state and time-resolved fluorescence emission studies in solution and as a thin film point towards the strongly quenched fluorescence emission and lifetime decay, suggesting that energy transfer occurs from the singlet excited state of Zn(II)-porphyrin unit to GO sheets.

1. Introduction

Graphene is rapidly becoming one of the most popular materials since its discovery by Geim *et al.*[1] The atomically thin, 2D structure that consists of sp2-hybridised carbons allows a remarkable electronic and mechanical properties.[2-5] These properties place graphene in a leading position as the next-generation material in the applications of nanoelectronic devices, including future photovoltaics, transparent conductive films, electrical energy storage and biosensors.[6-10] Chemical reduction of graphene oxide seems the simplest way to generate graphene in bulk, with yields suitable for further sustainable chemistry applications due to the low cost and little requirements for complex equipment.[11-13] And, there is increased interest in developing new chemistry of as-prepared graphene oxide, in particular, its supramolecular chemistry.

Graphene oxide (GO), a graphene derivative more accessible ready for chemical derivatization can be obtained by the controlled oxidation of graphite and has been recently studied in the context of sustainable chemistry applications.[14]

The electronic and mechanical properties of graphene oxide remain significantly inferior to those of pure graphene, but since it is more amenable to chemical derivatization and bulk production under sustainable conditions, this material is promising as a transparent conductive film material. Hence, there is significant merit in developing new functionalization techniques to manipulate its electronic properties and render it a suitable synthetic scaffold for applications in optical electronics. Due to the desirable electrical, optical and mechanical properties of GO and its chemical similarities to pure graphene it also has potential applications in photovoltaic materilas design.

The existence of numerous oxygenated species at the basal planes of graphene sheets renders it amenable for the formation of stable aqueous dispersions and

derivatization based on non-covalent and covalent interactions. The spectroscopic characteristics of GO are tunable and can be adjusted with the changes in the percentage of oxygen groups on its surface and the number of layers available in the dispersed phase. The oxygen containing groups include: –COOH, –OH and -O- functionalities which complement an extended π-aromatic network despite numerous disorder/defects regions, rendering this particularly effective at engaging in supramolecular interactions through aromatic staking reinforced by H bands.

Fluorescence measurements also demonstrate that graphene oxide hybrid materials can exhibit strong fluorescence, which absorb strong blue light at 392 nm, 414 nm and 438 nm and maintain a relatively high quantum yield[15] depended on the nature of the dispersing agent used in hybrid formation. Graphene oxide has been recently functionalized with small molecules giving rise to new materials: for example GO was found to bind strongly to p-phenylene diamine which was recently used as a dispersing agent.[16]

Porphyrins are planar, electron-rich, highly aromatic materials, characterized by remarkably high extinction coefficients in the visible region. These have been used in some recent studies as chromophores having the ability to act as dispersing agents on basis of their ability to π-π stacking with extended aromatic systems, such as carbon nanotubes[17] and nanohornes[18] for the development of prototype artificial photosynthetic devices.[19] However, functionalization of graphene nano-flakes with bulky and functional, tailor made porphyrins (either covalently and non-covalently) has not been explored thus far. There are so far only limited investigations into GO and porphyrin aggregates, and none involving aryl substitute functional porphyrins.

Here, we synthesized a novel porphyrin-based nanohybrid whereby the entire surface of graphene oxide was modified via supramolecular functionalization of carbon sheet graphene oxide. Due to its enhanced solubility in common organic solvents and lab-scale

availability via this validated synthetic route, a GO-aryl thioacetate-functionalized hexyl substituted Zn(II)-porphyrin was used. The Zn(II) complex resulted from the metalation of the corresponding free-base porphyrin, a member of a family of substituted porphyrins known to be soluble in most common solvents e.g. toluene, chloroform and ethanol.[20] This is of the interest as uniform dispersions of such graphene oxide nanohybrids may be used as thin layered materials with applications as scaffolds for future nano-optoelectronic devices.

2. Results and discussion

For the synthesis of the free base porphyrin and Zn(II)-porphyrin on a laboratory (milligram) scale suitable for further synthetic manipulations, the general procedure devised by Twyman and Sanders[21] was adapted and the details of the fully revised and validated protocol are shown in **Scheme 1**. This method involved the synthesis of 1-iodohexane, pentane-2,4-dione and benzyl 3-oxobutanonate as the starting materials.[22] The hexyl derived pyrrole acted as the basic building unit to build up porphyrins.[23,24] The side groups of the porphyrin and the metal center can be further tuned to incorporate several substituents for future photovoltaic devices. The free base porphyrin and Zn(II)-porphyrin has been specifically designed to incorporate four hexane chains on the side of the macrocycles allowing a suitable solubility in common organic solvents and facilitates purification. The molecular structure and supramolecular architecture of the free base porphyrin unit was determined in the solid state by single crystal X-ray crystallography (**Figure 1**). This single crystal was obtained from $CHCl_3$: MeOH solutions over several months. The free base porphyrin molecules are oriented face-face and show two heptane chain groups placed anti with respect to the aromatic core. The free base porphyrin supramolecular structure shows weakly linked tubular arrangements in the solid state. Furthermore, Ga (III), In (III)

and Fe (III) metalloporphyrin were synthesized, but due to the low yield, Zn (II) complex was chosen for characterization.

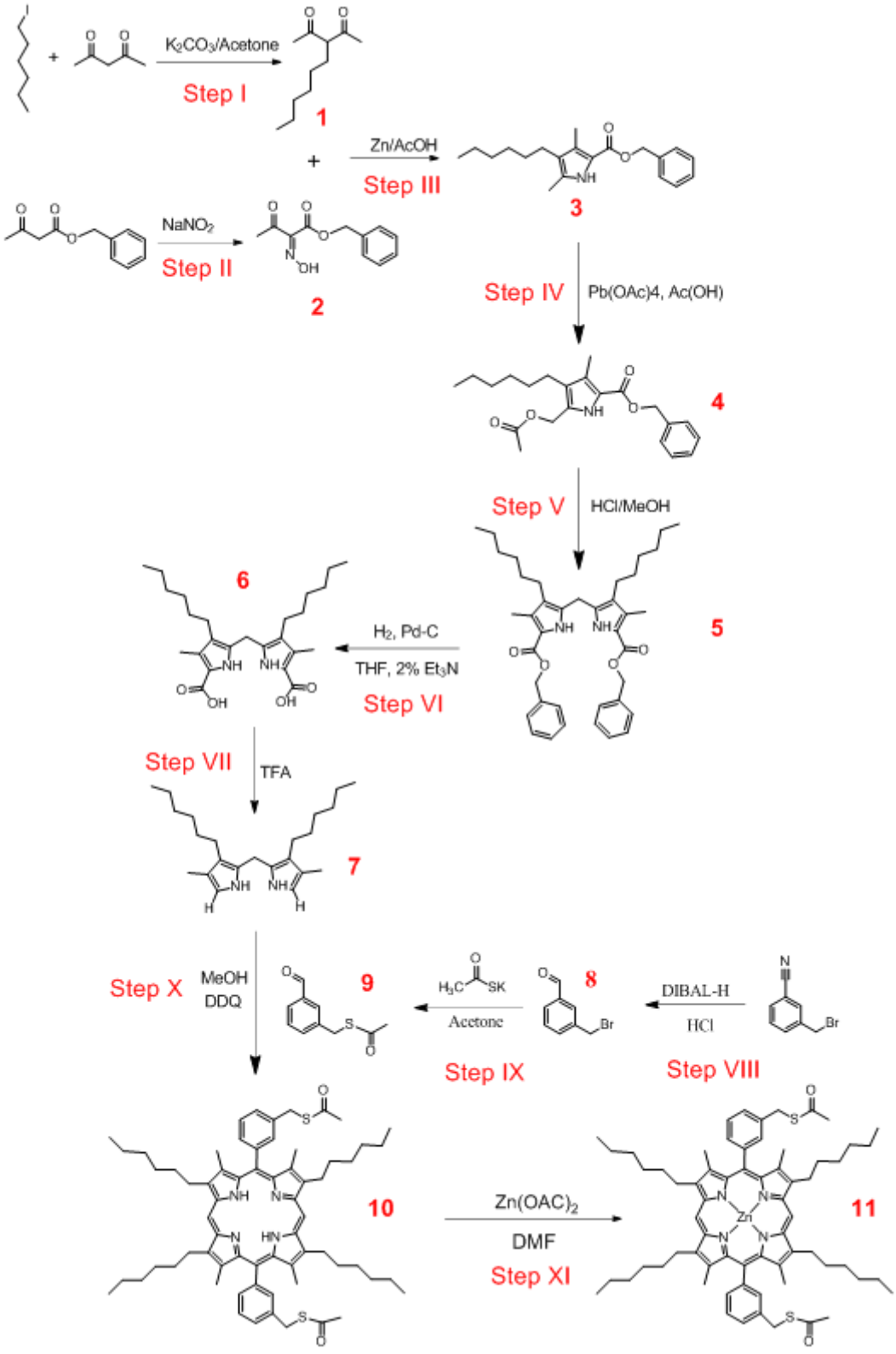

Scheme 1. General procedure used for the synthesis of the Zn(II) porphyrin

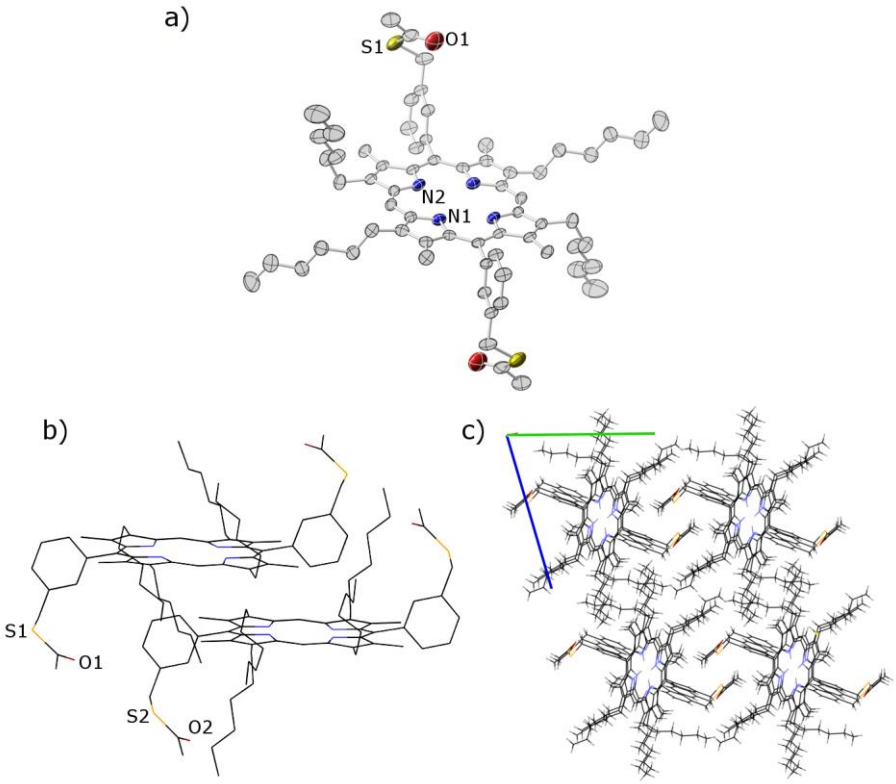

Figure 1. Molecular structure determinations by single crystal X-ray diffraction: a), b) Aceyl-protected free based porphyrin studied, showing two monomers in an aromatic stacking and c) cell packing diagram, view over axis *a*

Figure 2 shows the schematic diagram used for the generation of Zn(II)-porphyrin@GO complex. Since the graphene oxide was prepared by a modification of the known Hummers' method, oxygen functional groups such as hydroxyl, epoxyl, carboxyl and other carbonyl groups were likely present on the edge and on the surface of the graphene oxide sheets. As a result, following treatment by sonication, graphene oxide sheets can be efficiently exfoliated from the graphite oxide starting materials. The resulting graphene oxide and Zn(II)-porphyrin were suspended in ethanol, and stirred for 24 hours at room temperature. The resulting Zn(II)-porphyrin@GO nanohybrid material formed stable dispersions in ethanol (without precipitation over several weeks) and have been characterized by UV-vis, FT-IR and Raman. The treatment of the synthesized GO with the thioacetate Zn(II) porphyrin resulted in the

decoration of the surface of the graphene oxide and gave rise to a new nanohybrids denoted Zn(II)-porphyrin@GO (i.e., *porphyrin-GO complex*), @ is used as a distinctive to indicate that it is a composite material not only a combination of the two components.

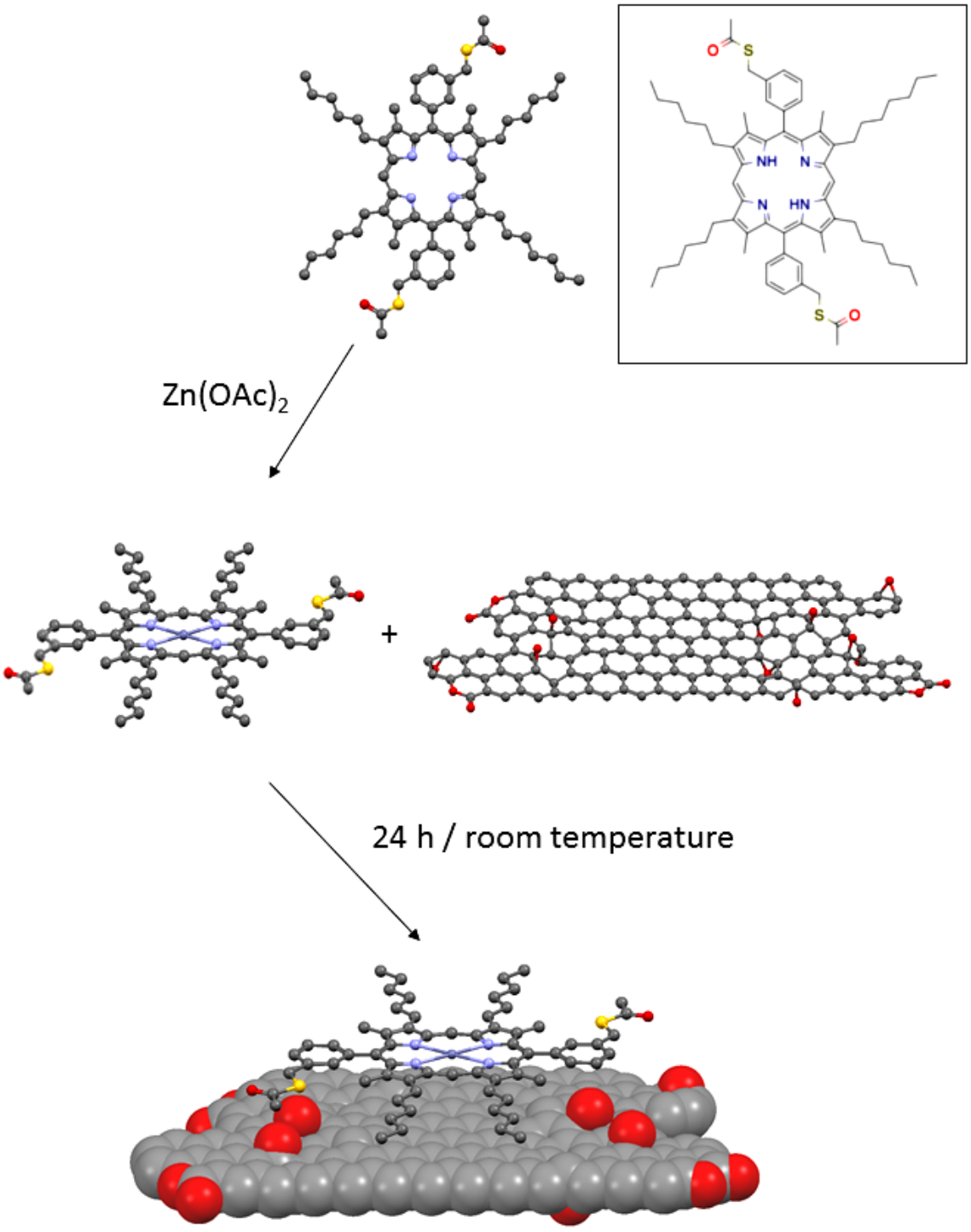

Figure 2. Schematic representation of the formation of a new of Zn(II)-porphyrin@GO complex.

The Zn(II)-porphyrin@GO complex was formed by π-π stacking between the pyrrole rings of the Zn(II)-porphyrin and the hexagonal rings on the graphene oxide sheets, likely reinforced by hydrogen bonding between –COOH or -OH groups of the GO and the –C=O unit of the thioacetate group. The further formation of Zn-O bond, between the Zn center from the porphyrin and the oxygen from the –COOH or –OH groups of the GO, cannot be discarded. The oxygen will occupy the fifth coordination position of the Zn center. The morphology of Zn(II)-porphyrin@GO nanohybrid was compared to that of the original GO material determined by AFM and TEM /SAED. Steady-state and time-resolved fluorescence emission studies have been carried out to probe whether or not an energy transfer occur between graphene oxide nano-flakes and the Zn(II)-porphyrin layers.

The direct observation of Zn(II)-porphyrin@GO layered material in the solid state was carried out by TEM microscopy combined with energy dispersive X-ray spectroscopy analysis. TEM images, shown in **Figure 3**, indicates that graphene oxide has a sheet-like structure. The selected area electron diffraction (SAED, **Figure 3b**) indicates a crystalline structure. This means that the graphene oxide sheets are rotation oriented with each other and the properties of each layer are unique as expected. The interlayer coherence is not destroyed in the EtOH dispersion used. TEM and AFM showed that following complexation with Zn(II)- porphyrin, the graphene oxide sheets form uniform, multi-layer Zn(II)-porphyrin@GO aggregate structure (**Figure 3c** and **3d**). **Figure 3d** represents a typical TEM micrograph of Zn(II)-porphyrin@GO hybrid material. **Figure 3d** exhibits more detailed surface information of the Zn(II)-porphyrin@GO complex: the Zn(II)-porphyrin molecules are tightly attached on the

whole surface area of graphene oxide and it appears that Zn(II)-porphyrin forms nanocrystalline structures. The EDX indicates the presence of Zn elements and the complexation of the complex structure of the Zn(II)-porphyrin.

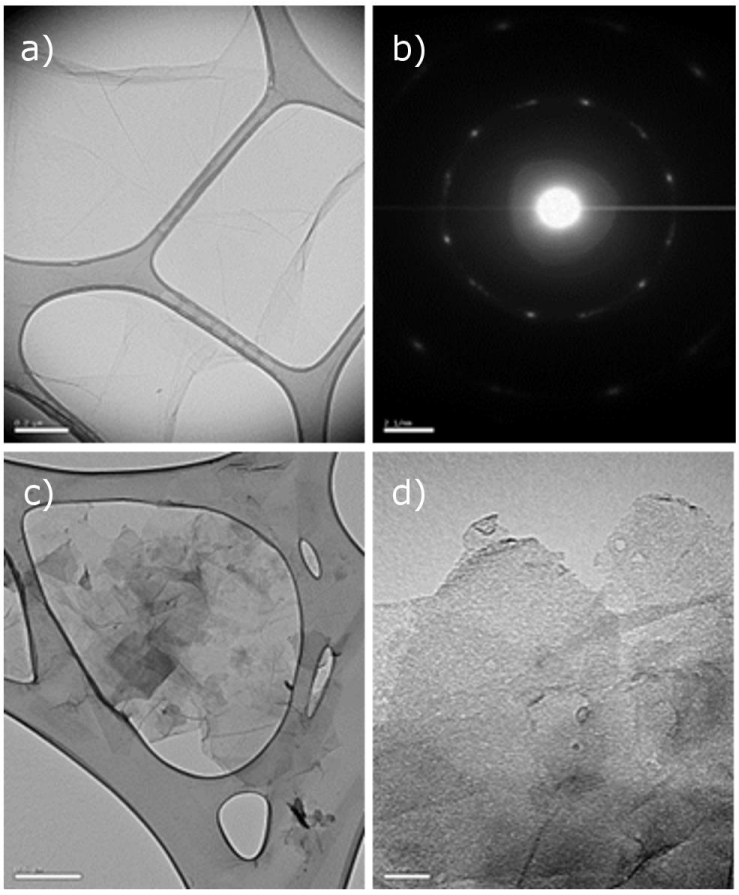

Figure 3. a) TEM micrograph of graphene oxide (bar = 200 nm); b) SAED of graphene oxide, the scale (bar = 2 nm^{-1}); c) TEM image of Zn(II)-porphyrin@GO complex (bar = 500 nm); d) Magnified TEM area from Fig 3c, Zn(II)-porphyrin@GO complex (bar = 50 nm)

The Zn(II)-porphyrin AFM sample was prepared by using spin coating at 3000 rpm speed coated Zn(II)-porphyrin solution (0.02 mg/mL) on 2 cm^2 Muscovite Mica substrate. It can be seen from **Figure 4a** and **Figure 4b** that the Zn(II)-porphyrin molecule does not wet the surface well as it dries to form uncrystallized islands the heights of which are around 10 nm. Due to the presence of porphyrin as a modification

of the native GO surface, the stabilized solution forms islands with a high contact angle indicating a double layer repulsion.

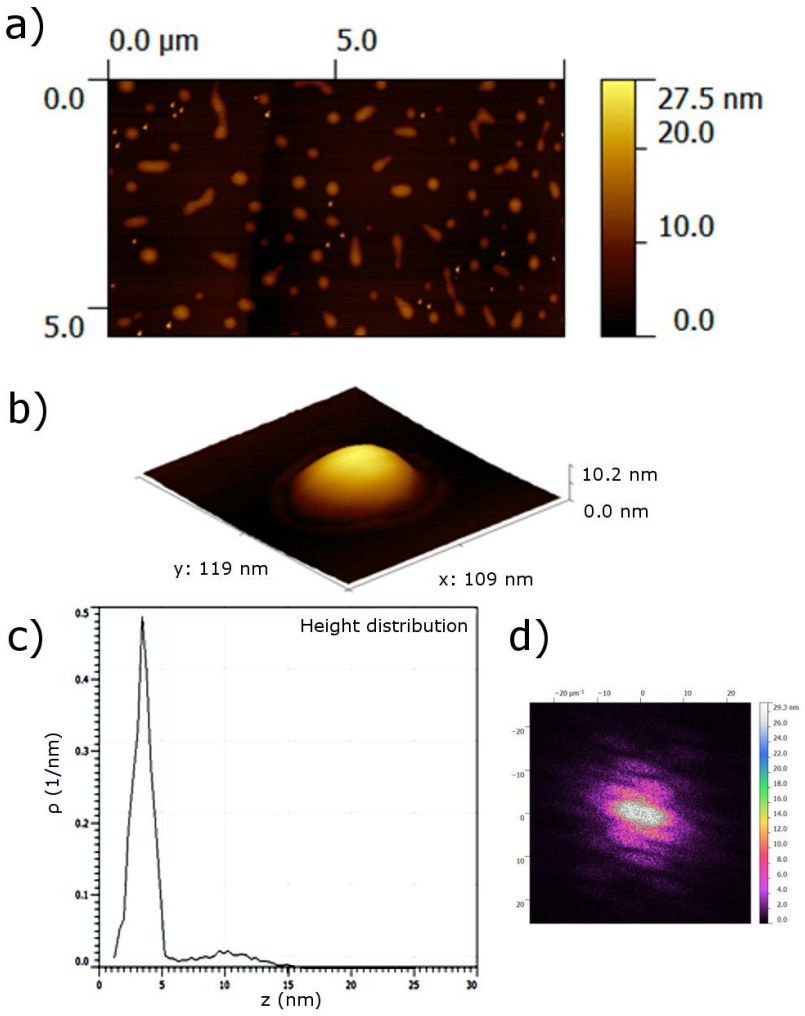

Figure 4. a) AFM image of intact Zn(II)-porphyrin self-assembly on a Muscovite Mica substrate by 3000 rpm spin coating b) 3D Tapping mode AFM image of Zn(II)-porphyrin self-assembly crystal, c) profile analysis showing the heights of distribution curve in the mica substrate d) the image of two dimensional FFT

The Zn(II)-porphyrin@GO AFM sample was generated by dropping Zn(II)-porphyrin@GO solution on O_3-Modified Highly Ordered Pyrolytic Graphite (HOPG) substrate. **Figure 5a** and **Figure 5b** show that the Zn(II)-porphyrins form regular semi-triangular tiny crystal structures on the surface of graphene oxide.

The insert fast Fourier transform (FFT) shows that this regular semi-triangular structure is crystalline, which confirms the observation from the TEM images. From **Figure 5c**, the file of heights of distribution curve analysis, it can been seen that the heights Zn(II)-porphyrin@GO are around 2-3 nm. Considering the height of a single GO sheet[25] as 0.8-1 nm and the additional contribution from the attached Zn(II)-porphyrin crystal structure, the obtained images are characteristic of single and/or bilayers of exfoliated GO sheets and representative the different batches of GO used as-synthesized. The AFM image of the Zn(II)-porphyrin@GOs also indicates that the Zn(II)-porphyrin was uniformly and regularly deposited onto the entire surface area of GO as well as strongly bond. The difference between dewetting Zn(II)-porphyrins and semi-triangular Zn(II)-porphyrin confirms a consequence of the adsorptive interaction between Zn(II)-porphyrins with graphene oxides through π-π stacking and the formation of a Zn(II)-porphyrin@GOs complex.

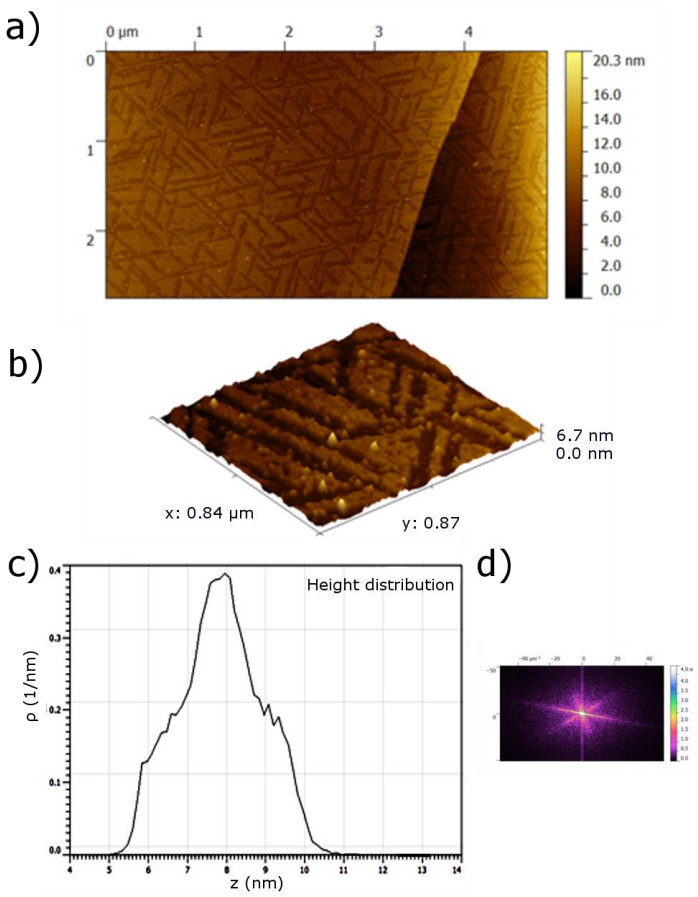

Figure 5. a) Tapping mode AFM image of Zn(II)-porphyrin@GO complex by doing complex solution onto an Ozone modified HOPG substrate b) 3D Tapping mode image of Zn(II)-porphyrin@GO complex, c) profile analysis showing the heights of distribution curve d) image of two dimensional FFT

Raman spectroscopy is widely used in characterization of carbon nanomaterials given its ability to inform on vibrational and other low-frequency modes in such systems.[26,27] The Raman spectra shown in Fig. 6 were recorded for dispersed samples deposited from ethanol using a laser excitation of 514 nm, a region of the emission spectra of the Zn(II)-porphyrin@GO without interference from fluorescence emission from Zn(II)-porphyrin. It can be seen from **Figure 6** that the pure graphene oxide exhibits a D band peak at 1350 cm^{-1} due to carboxylic group on the sheet edges and oxidized defects or disordered carbon on the surface.[28]

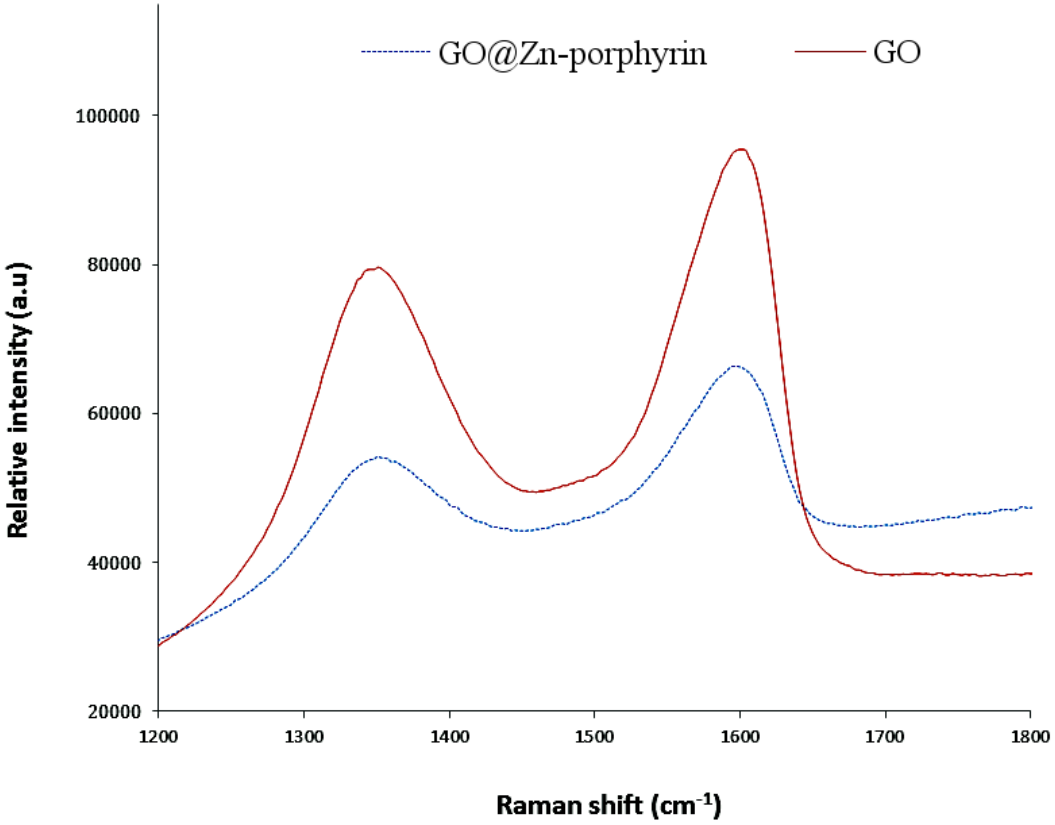

Figure 6. Raman spectroscopy of GO and Zn(II)-porphyrin@GO

It also exhibits a G band peak at 1599 cm^{-1}, which corresponds to sp^2-bonded carbon structure.[26] The I_d/I_g ratio of pure graphene oxide is 0.834. It is well known that an increased ratio of I_d/I_g indicates a lower degree of crystallinity of graphite type materials.[29] The π-π stacking interaction can occur between Zn(II)-porphyrin and graphene oxide sheets due to the additional π-π stacking and the anchoring of phenyl rings. When the Raman spectrum of pure GO was compared to that of Zn(II)-porphyrin@GO complex it was found that the D band peak of Zn(II)-porphyrin@GO complex is located at 1350 cm^{-1} while the G band peak of Zn(II)-porphyrin@GO complex is shifted slightly down to 1596 cm^{-1}, possible caused by the decreased number of layers in their solid states. This might be due to the longer sonication time (120 min) needed to be used to form the Zn(II)-porphyrin@GO material. The ratio of I_d/I_g of Zn(II)-porphyrin@GO is 0.817. According with literature, the change in this value with respect to pure graphene oxide, indicates that some of the oxygenated functional groups from Zn-porphyrin molecules and/or the Zn-O of the GO interaction participate in the network of conjugated graphene layers.[30]

Two-dimensional fluorescence contour plotting for the free graphene oxide (**Figure 7a**), free base porphyrin (**Figure 7b**), GO@free base porphyrin (**Figure 7c**), intact Zn(II)-porphyrin (**Figure 7d**) and Zn(II)-porphyrin@GO (**Figure 7e**) were recorded separately (scanning every 10 nm, λ excitation from 200 nm to 800 nm, λ emission from 200 nm to 800 nm) to investigate the excitation and emission behavior differences of free base porphyrin and Zn(II)-porphyrin before and after complexation with graphene oxide. A strong, broad, emission peaks, from 590 nm to 700 nm and from 550 nm to 670 nm was observed from free base porphyrin and Zn(II)-porphyrin 2D fluorescence contour plotting respectively due to changes occurring in the porphyrin molecular structure after metalation. Following the complexation between

graphene oxides and Zn(II)-porphyrin in ethanol, it can be seen that significant amount of free Zn(II)-porphyrins was absorbed onto graphene oxide, whilst strong Zn(II)-porphyrin peaks disappeared from the Zn(II)-porphyrin@GO contour plot. The plot also shows that the emission wavelength of the peak maximum, experience a slightly red-shift (30 nm for the maximum). The plots additionally indicate that the intensity of Zn(II)-porphyrin was severely quenched after complexation with graphene oxide. A similar behavior regarding quenching of fluorescence and strong red-shift appeared at the complexation between free base porphyrin and graphene oxide. These red-shifts and quenching are consequences of strong π-π donor-acceptor interactions occurred as a result to link porphyrin molecules and graphene oxides together and the energy transport from the singlet excited state of Zn(II)-porphyrin to graphene oxide.

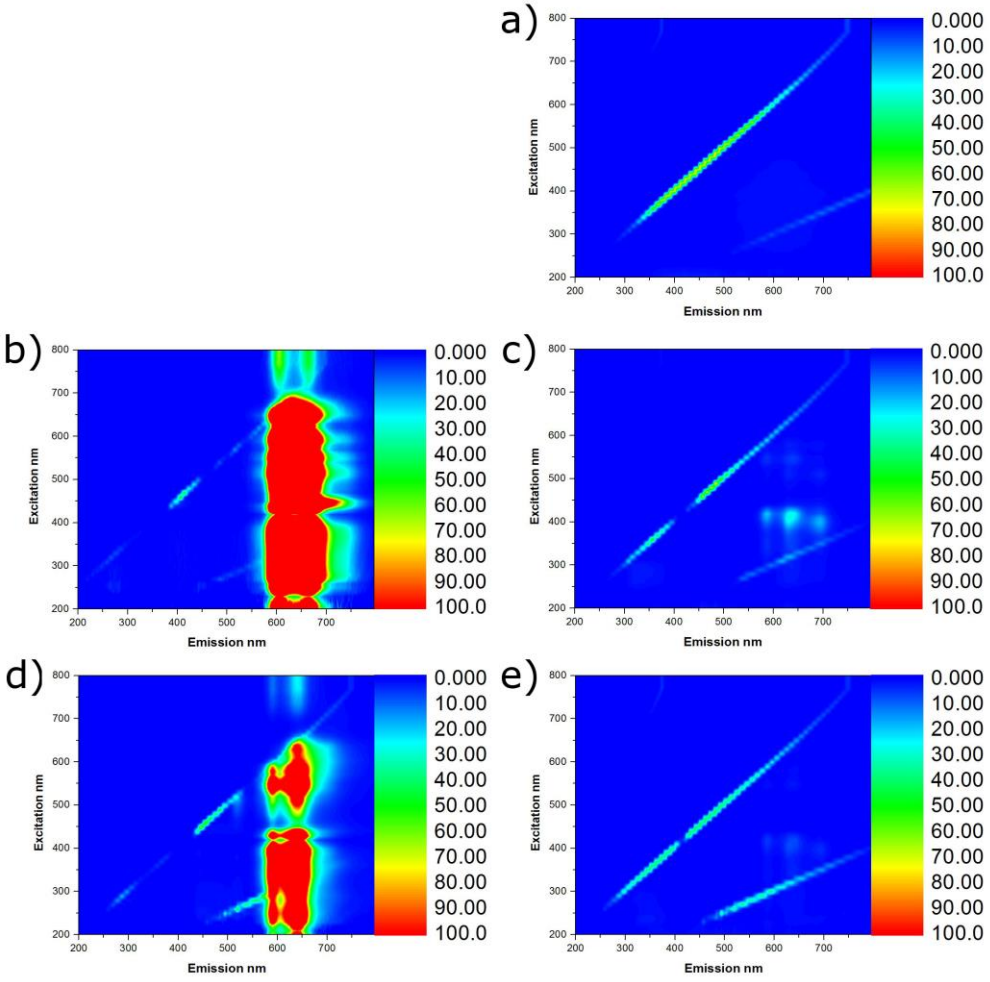

Figure 7. Normalised two-dimensional fluorescence contour plots recorded for dispersions of: a) Free graphene oxide in ethanol (0.5 mg/mL); b) Free base-porphyrin in ethanol (1 μM); c) Pure graphene oxide (0.5 mg/mL) and free base porphyrin (1 μM) mixture in ethanol; d) Zn(II)-porphyrin in ethanol (1 μM); e) Pure graphene oxide (0.5 mg/mL) and Zn(II)-porphyrin (1 μM) mixture in ethanol

Optical absorption and fluorescence emission measurements were also carried out using UV-visible spectroscopy and fluorescence spectroscopy. **Figure 8** shows the optical absorption spectra of Zn(II)-porphyrin dispersed in ethanol (3 mL, 1μM) , then titrated with Zn(II)-porphyrin (0.5 μM) and graphene oxide (0.05 mg/mL) ethanol solution. It can be seen from **Figure 8a** that the main Zn(II)-porphyrin absorption peak at 416 nm was enhanced when added graphene oxide solution was added. **Figure 8b** shows that the absorption behavior increased logarithmically with the concentration of graphene oxide. Same measurement conditions were also applied to Zn(II)-porphyrin and graphene oxide fluorescence spectroscopy measurement with λ_{ex}=346 nm, from **Figure 8c**, the main emission peak at 438 nm was quenched when graphene oxide solution was added. **Figure 8d** shows the normalized emission intensity with respect to added volume of the graphene oxide. The UV-vis enhanced behavior and Fluorescence quenched behavior might be a consequence of the electronic interactions between Zn(II)-porphyrins and graphene oxide in the ground state, which indicates the complexation of Zn(II)-porphyrin@GO complex.

Although by UV-visible measurements (**Figure 8b**) it is not possible to observe in a clear way a critical point suggesting a cooperative aggregation model,[31] due to the shape of the curve. This aggregation behavior is confirmed by the fluorescence studies. In **Figure 8d** a critical point about 530 μL (0.265 mg of GO was added) is observed, which indicates cooperative aggregation model. A possible explanation of the absence of this critical point in UV-visible measurements may be due to the UV-vis absorption

processes, in this case, are less affected by the interaction between the products than fluorescence absorption-emission processes.

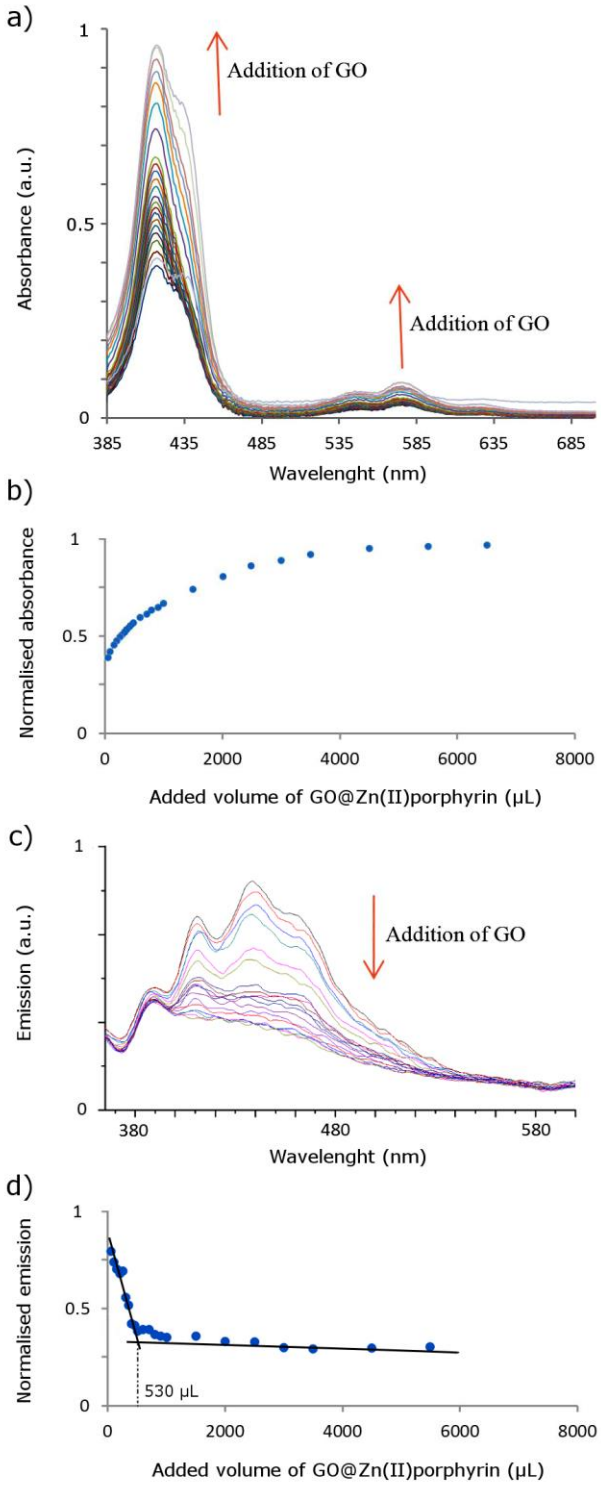

Figure 8. a) UV-visible absorption enhancement behavior in the spectroscopy of Zn(II)-porphyrin@GO. b) UV-visible absorption normalized intensity with respect to

added volume of the graphene oxide. c) Fluorescence emission quenching behavior in Zn(II)-porphyrin@GO spectroscopy. d) Fluorescence emission normalized intensity with respect to added volume of the graphene oxide. Linear fit in Origin 9.0 using statistical model.

A number of fitting protocols were applied to facilitate establishing a bonding model and a job plot but, given GO is a non-linear disordered material these fitting models were not reliable. However, based on the quenching of fluorescence the interaction between the Zn(II)-porphyrin and the GO is clear.

In the graphene oxide FTIR spectrum (**Figure 9**) prior to complexation, the bands at 1095 cm^{-1} and 1759 cm^{-1} are due to C=O stretching vibrations from carbonyl and carboxylic groups and the band located at 1612 cm^{-1} is due to C-OH stretching vibration. Thus, FTIR spectroscopy provided evidence of the presence of an abundance of different types of oxygen functionalities on the surface. The peak at 881cm^{-1} for Zn(II)-porphyrin almost disappears compared to the Zn(II)-porphyrin@GO complex FTIR spectrum. In contrast to the GO and Zn(II)-porphyrin@GO spectra, a new broad band emerges at 1264 cm^{-1}, which corresponds to the C-N stretching band of the amide

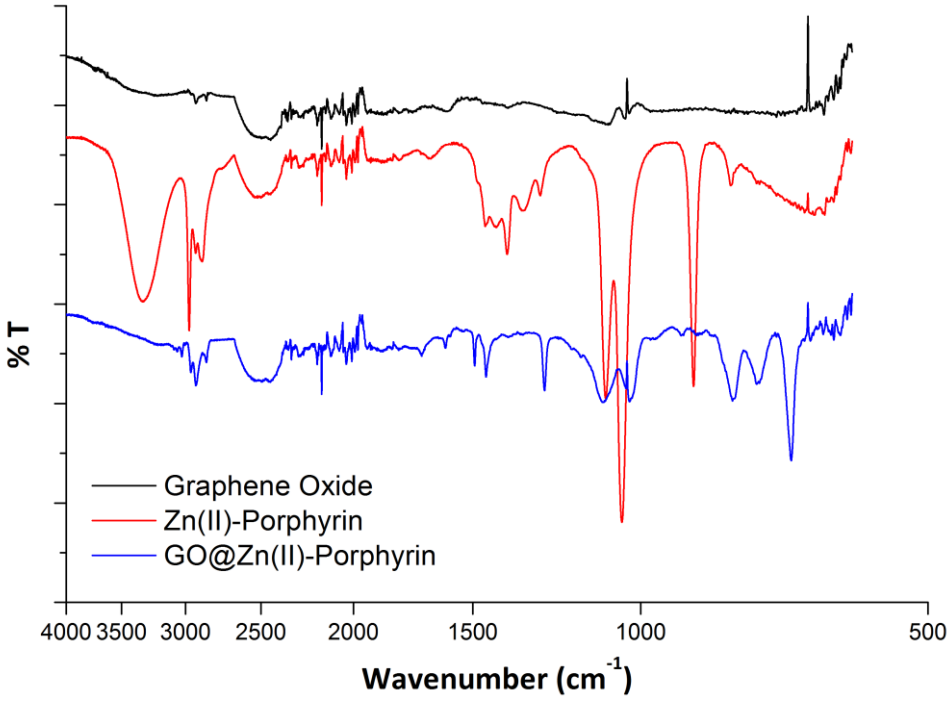

Figure 9. Overlay of the FTIR spectra of GO, Zn(II)-porphyrin and Zn(II)-porphyrin@GO

group. The peaks at 1456 cm^{-1}, 1495 cm^{-1} and 1630 cm^{-1} are representative of carboxylate groups. The peak observed at 1711 cm^{-1} is the C=O stretching vibration. These results suggest a successful non-covalent attachment of graphene oxide and Zn(II)-porphyrin.

In order to further study the interaction between graphene oxide and Zn(II)-porphyrin in the excited state (dispersed phase and thin film), fluorescence excited state life was performed using time correlated single-photon counting. From the fluorescence decay time-profiles shown in **Figure 10**, the fluorescence lifetimes of photo excited porphyrin in the Zn(II)-porphyrin@GO complex were fitted and gave a two component lifetimes of 0.8 ns (75.2%) and 3.7 ns (24.8%) with a good χ^2 of 1.27 in Zn(II)-porphyrin@GO complex fitted curve and χ^2=1.22 for the Zn(II)-porphyrin. These values are significantly lower than that of the intact porphyrin, 6.8 ns. It is reasonable therefore to assumed that there is a charge-separation and/or energy transfer process in the Zn(II)-porphyrin@GO complex. In addition, the result also supports an efficient emission quenching of the Zn(II)-porphyrin when added to graphene sheets, which was observed in two-dimensional fluorescence contour plotting in **Figure 5**.

Figure 11 show lifetime emission maps for the solid-state Zn(II)-porphyrin and Zn(II)-porphyrin@GO composite together with single-photon induced fluorescence intensity maps showing the spatial variations in fluorescence emission lifetimes. The lifetime imaging maps and corresponding distribution plots for the predominant lifetime component (τ1) for Zn(II)-porphyrin and Zn(II)-porphyrin@GO composite.

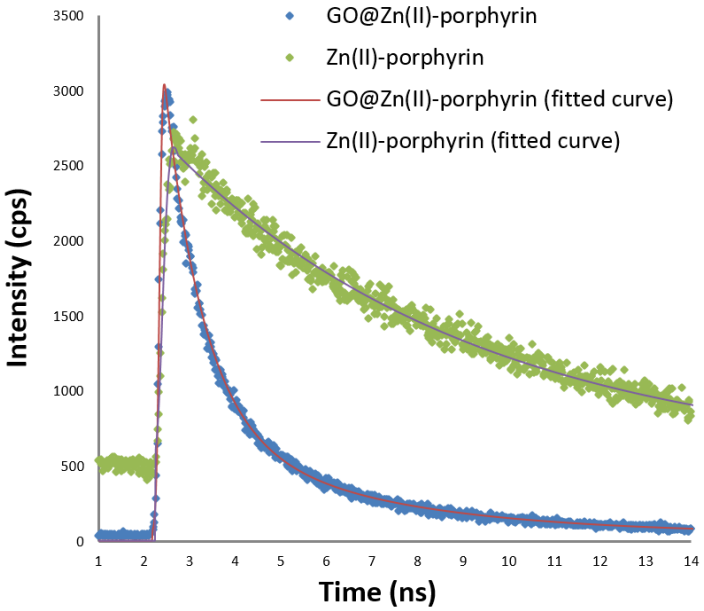

Figure 10. Single-photon fluorescence lifetime spectroscopy (λ_{ex}=473 nm, Zn(II)-porphyrin 1 μM dispersion in ethanol, Zn(II)-porphyrin@GO complex dispersion containing 1μM porphyrin and 0.1 mg/mL graphene oxide.[32]

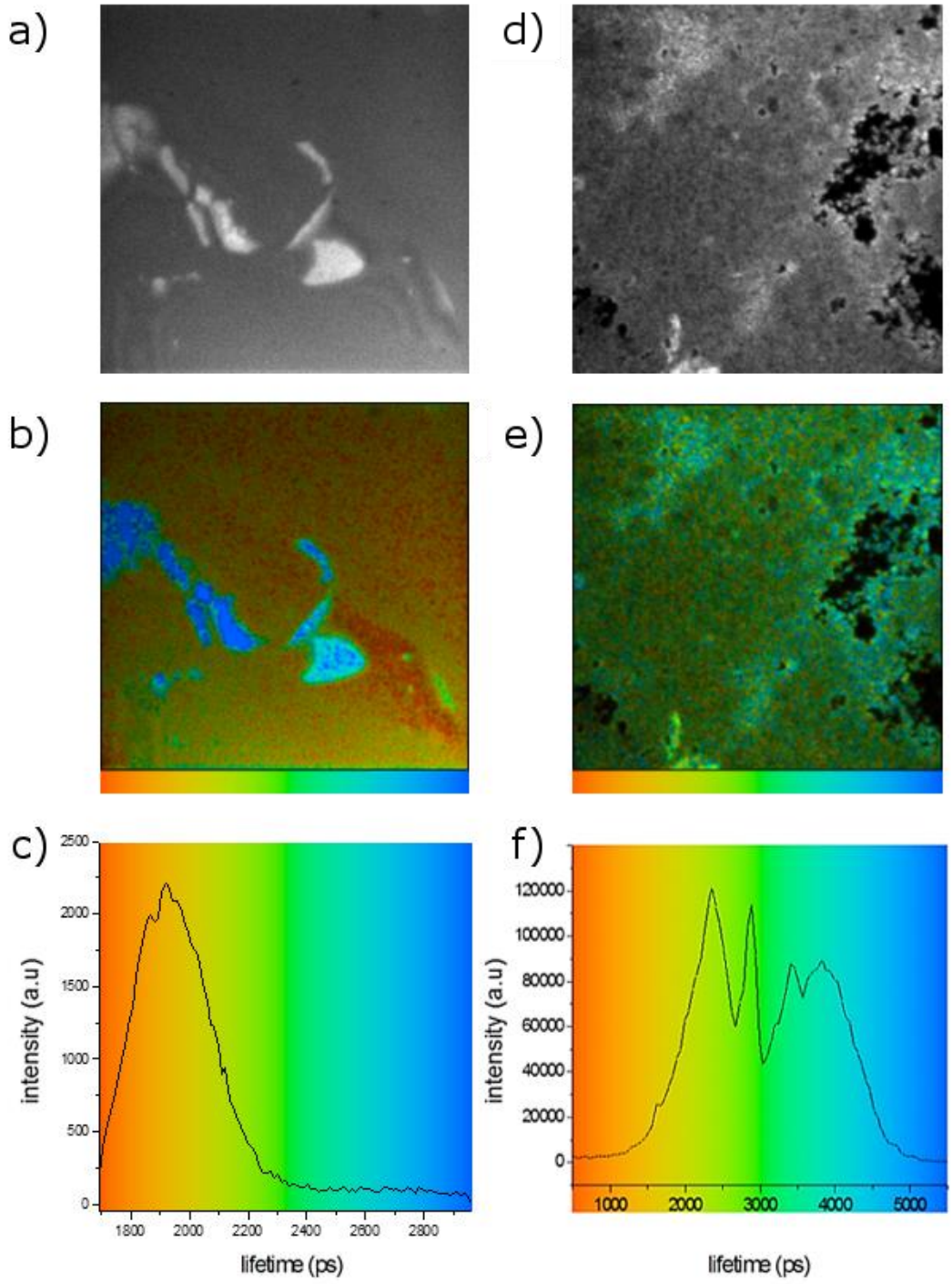

Figure 11. Representative single-photon laser confocal fluorescence of a thin film obtained by drop casting a solution of nanohybrid onto borosilicate glass: (a) solid Zn(II)-porphyrin, intensity image, (b) lifetime mapping (c) corresponding fluorescence lifetime distribution curve of Zn(II)-porphyrin and scalebar, (d) solid Zn(II)-porphyrin@GO composite, intensity image, (e) lifetime mapping and (f) corresponding fluorescence lifetime distribution curve and scalebar.

From **Figure 11a** and **11b**, it can be seen that some solid-state Zn(II)-porphyrin tend to be self-aggregate together (deep blue part in Fig. 11b) to form a high concentrate structure. This self- aggregated behavior lead to the major lifetime components measured in self- aggregated Zn(II)-porphyrin were 2500±300 ps, while the major lifetime components measured in other Zn(II)-porphyrin were 1900±100 ps in **Figure 11c**. The major lifetime components measured in Zn(II)-porphyrin@GO composite were 2300±300 ps and 3800±100 ps form **Figure 11f**. A comparatively broader FWHM (full width at half of the maximum) of the lifetime distribution, namely 3000 ps, indicated the low homogeneity of fluorescence decay and that this composite has a hybrid structure, where the ns lifetime decay profile of the free porphyrin is clearly identified, yet modified by the close proximity of the GO: this environment (acting as a 'nano-host') clearly influences the spectroscopic behavior of the porphyrin.

3. Conclusion

In this article, Zn(II)-porphyrin and graphene oxide sheets were non-covalently assembled giving rise to a new Zn(II)-porphyrin@GO complex material. This can be synthesized in bulk following the oxidation of graphite and subsequent supramolecular functionalization with a functional Zn(II)-porphyrin especially selected on basis of its solubility in organic solvents. The structure and morphology of Zn(II)-porphyrin@GO hybrid material have been studied by XRD, AFM, TEM coupled with SAED and fluorescence lifetime measurements. It can be seen that the Zn(II)-porphyrin forms nano-crystalline structures when deposited onto the surface of graphene oxide sheets, which exhibit different morphology compared to the self-assembly of the free Zn porphyrin onto the same surfaces in the absence of GO. Raman spectroscopy showed the structure and surface information of graphene oxide and Zn(II)-porphyrin@GO

complex and corroborated with optical absorption and FT-IR studies confirm the conjugation of Zn(II)-porphyrin and graphene oxide sheets. The fluorescence quenching and florescence lifetime decay suggests that a strong electronic interaction between Zn(II)-porphyrin and graphene oxide occurs in the excited state. This interaction is likely due to the energy transfer from Zn(II)-porphyrin to the graphene oxide, which can potentially be used in the construction of novel optoelectronic devices with graphene oxide as a strong electron acceptor. Overall we have fully characterized graphene-based hybrid materials possessing non-covalently linkages with soluble porphyrins towards the development of novel optoelectronic devices. This is the first time where a graphene analogue derivative was functionalized with a tailor-made lab-scale synthesized porphyrin on a practical scale suitable for extended spectroscopic and imaging analysis investigations.

4. Experimental Section

Synthesis of graphene oxide: Graphene oxide sheets were exfoliated from graphite oxide using an adapted procedure from the published Hummers methods.[33] The graphite oxide was generated from natural graphite powder (SP-1 grade 325 mesh, Bay Carbon Inc.). 10 g of powdered flake graphite and 5 g of sodium nitrate were stirred in 230 mL technical concentrated sulfuric acid in a 1.5L beaker. This beaker was then rested on an ice bath to maintain the temperature at 0 ℃. Under stirring, 30 g of potassium permanganate were added into this mixture. The rate of addition was controlled carefully so that the temperature of the mixture did not exceed 20 ℃. The reaction was then removed from the ice bath and the temperature was allowed to rise to 35℃. The mixture was then stirred at room temperature for a further 30 min. 460 mL of distilled water were slowly added into the mixture, and it was observed that the temperature of the mixture increases and causes effervescence to occur. Then, the mixture was diluted to approximately 1.4 L with distilled water. An aqueous

solution of 3% H_2O_2 was slowly added into the mixture to remove excess permanganate and manganese dioxide. Afterwards, the color of the suspension became bright yellow. The suspension was filtrated whilst still warm, and then rinsed with excess warm water. A filtration step followed and the solid was collected onto the Cyclopore membrane followed by dispersion in 3.2 L distilled water. A two week dialysis process was then introduced to remove any remaining salts. Afterwards, the suspension was filtrated again and rinsed with distilled water. The solid fractions were collected from the filtering membrane. The solid products were then kept at 60℃ in a furnace overnight to make sure the graphite oxide was fully dried. For the preparation of graphene oxide dispersions in the dried product it was diluted with ethanol to make 2% w/v dispersion. The suspension was sonicated in an ultrasonic bath (40 kHz) for 3 h, which was separated into 6 x 30 min sonication sessions with 10 min intervals between each session. The suspension was then centrifuged at 3000 rpm for 30 min. The supernatant was taken and was found that it may remain free of precipitation when allowed to settling for a minimum of 1 month. After this period, a microfiltration was performed and only the clear supernatant was used in the experiments. This lengthy procedure was deemed necessary, and repeated several times to secure batch-to-batch consistency of the resulted GO material. This was tested by IR spectroscopy and compared to the corresponding spectra of graphite and graphite-oxide.

Synthesis of the complex Zn(II)-porphyrin@GO: The clear and stable graphene oxide solution emerging from the process described above was introduced into a filtration process and the graphene oxide solid was collected from the membrane filter. A sample of 5 mg graphene oxide was suspended into 50 mL of ethanol. The mixture was treated with 3 × 10 min of sonication which had 5 min intervals between each section to make sure that the graphene oxides were fully dispersed. A solution of Zn(II)-porphyrin was prepared by adding 1 mg protected Zn(II)-porphyrin to 50 mL of ethanol. Afterwards, the Zn(II)-porphyrin solution was added to the graphene oxide dispersion to obtain the Zn(II)-porphyrin@GO

complex. The mixture was stirred for 24 hours. Subsequently, the mixture was filtered and the solids on the membrane were rinsed with excess ethanol. Graphene oxides and Zn(II)-porphyrins complex were collected from the membrane filter. The complex was fully dried in a 60℃ furnace overnight. The final solid product was then ready to be characterized by spectroscopic methods and microscopy.

Materials characterization: A comprehensive examination of the obtained products was conducted using a broad set of characterization techniques. Transmission electron microscope (TEM) images were obtained with Gatan Dualvison digital camera on a JEOL 1200EXII transmission electron microscope coupled with Energy-dispersive X-ray spectroscopy (point resolution, 0.16 nm). Raman spectroscopy was carried out on a Renishaw inVia Raman spectroscopy. The specimens were either in solid state or dispersed in pure water (MilliQ) or water: ethanol 1:1 mixture. During the measurement, the carbon nanomaterials samples were deposited on an aluminum plate substrate. The input wavelength was set at 514 nm. More than 10 times accumulations were generally applied in Raman spectroscopy measurements, and the beam was focused in at least three different position across the specimen and these spectra were averaged to obtain batch-representative peaks and most reliable results. Fluorescence spectroscopy measurement was carried out on a Perkin Elmer Luminescence spectrophotometer LS 55. The concentration of sample applied to fluorescence spectroscopy can be vary between 10^{-5}-10^{-7} M depend on the strength of the fluorescence. UV-vis spectroscopy was carried out by using a Perkin-Elmer Lambda 35 spectrometer. The Atomic Force Microscopy measurement was carried out a Digital Instruments Multimode Atomic Force Microscope with IIIa controller. All AFM measurement were obtained under tapping mode and the measuring probes are Silicon Probes (Nascatec GmbH model NST-NCHFR). The AFM samples were deposited onto freshly cleared mica substrate by spin coating (Laurell Technologies WS-400, 3000rpm) or HOPG substrate depends on the sample dispersibility and

hydrophilicity. Fourier transform Infrared spectra were obtained by using a Perkin-Elmer 1000 FT-IR spectrometer.

Crystal structure determination: Crystals of acetyl-protected free based porphyrin were grown from THF and pentane mixtures. Crystal and structure refinement data are summarized in Table S1 (SI). Data were collected at 180 K on a Nonius Kappa CCD with graphite-monochromated Mo-K_α radiation (λ = 0.71073 Å). The structures were solved by direct methods using the program SIR92.[34] The refinement and graphical calculations were performed using the CRYSTALS[35,36] and CAMERON[37] software packages. The structures were refined by full-matrix least-squares procedure on *F*. All non-hydrogen atoms were refined with anisotropic displacement parameters. Hydrogen atoms were located in Fourier maps and their positions adjusted geometrically (after each cycle of refinement) with isotropic thermal parameters. Chebychev weighting schemes and empirical absorption corrections were applied.[38] [CCDC 1428500 contains the supplementary crystallographic data for this paper. These data can be obtained free of charge from The Cambridge Crystallographic Data Centre via www.ccdc.cam.ac.uk/data_request/cif.]

Fluorescence lifetime measurements: Fluorescence lifetime measurements using single-photon excitation experiments were performed at the Rutherford Appleton Laboratory under the supervision of Prof. S. Botchway (Central Lasers facility, Research Complex at Harwell). An optical parametric oscillator was pumped by a mode locked Mira titanium sapphire laser (Coherent Lasers Ltd), generating 180 fs pulses at 75 MHz and emitting light at a wavelength of 580-630nm nm. The laser was pumped by a solid state continuous wave 532 nm laser (Verdi V18, Coherent Laser Ltd), with the oscillator fundamental output of 473 ± 2 nm or 405 ± 2 nm. The laser beam was focused to a diffraction limited spot through a water immersion ultraviolet corrected objective (Nikon VC x60, NA1.2) and specimens illuminated at the microscope stage of a modified Nikon TE2000-U with UV transmitting optics. The focused laser spot was raster scanned using an XY galvanometer (GSI Lumonics). Fluorescence

emission was collected without de-scanning, bypassing the scanning system and passed through a colored glass (BG39) filter. The scan was operated in normal mode and line, frame and pixel clock signals were generated and synchronized with an external fast microchannel plate photomultiplier tube used as the detector (R3809-U, Hamamatsu, Japan). These were linked via a Time-Correlated Single Photon Counting (TCSPC) PCmodule SPC830. Lifetime calculations were obtained using SPCImage analysis software (Becker and Hickl, Germany) or Edinburgh Instruments F900 TCSPC analysis software.

Supporting Information

Supporting Information is available from the Wiley Online Library or from the author.

Acknowledgements

Prof. Jeremy K. M. Sanders FRS and the Sanders Group at Cambridge, as well as Dr Nick Bampos and Prof Sijbren Otto are acknowledged for training, helpful discussion in porphyrin synthesis and mentorship to SIP group. Drs Amy Kieran, Lok Tong and Rory Arrowsmith are thanked for involvement with initial stages of the porphyrin synthesis and characterization. SIP and SWB thank The Royal Society and STFC for funding. BYM thanks the University of Bath for a studentship (ORS).

Received: ((will be filled in by the editorial staff))
Revised: ((will be filled in by the editorial staff))
Published online: ((will be filled in by the editorial staff))

[1] A. K. Geim, K. S Novoselov, *Nature Mater.* **2007**, *6*(3), 183.

[2] D. Li, R. B. Kaner, *Science* **2008**, *320*, 1170.

[3] D. A. Dikin, S. Stankovich, E. J. Zimney, R. D. Piner, G. H. B. Dommett, G. Evmenenko, S. T. Nguyen, R. S. Ruoff, *Nature* **2007**, *448*, 457.

[4] J. S. Bunch, A. M. van der Zande, S. S. Verbridge, I. W. Frank, D. M. Tanenbaum, J. M. Parpia, H. G. Craighead, P. L.Mceuen, *Science* **2007**, *315*, 490.

[5] Y. Zhu, S Murali, W Cai, X Li, J. W. Suk, J. R. Potts, R. S. Ruoff, *Adv. Mater.* **2010**, *22* (46), 5226.

[6] X. Li, X. Wang, L. Zhang, S. Lee, H. Dai, *Science* **2008**, *319*, 1229.

[7] M. D. Stoller, S. Park, Y. Zhu, J. An, R. S. Ruoff, *Nano Lett.* **2008**, *8*, 3498.

[8] a) S. Stankovich, D. A. Dikin, G. H. B. Dommett, K. M. Kohlhaas, E. J. Zimney, E. A. Stach, R. D. Piner, S. T. Nguyen, R. S. Ruoff, *Nature* **2006**, *442*, 282; b) T. Ramanathan, A. A. Abdala, S. Stankovich, D. A. Dikin, M. Herrera Alonso, R. D. Piner, D. H. Adamson, H. C. Schniepp, X. Chen, R. S. Ruoff, S. T. Nguyen, I. A. Aksay, R. K. Prud'Homme, L. C. Brinson, *Nature. Nanotechnol.* **2008**, *3*, 327.

[9] P. Blake, P. D. Brimicombe, R. R. Nair, T. J. Booth, D. Jiang, F. Schedin, L. A. Ponomarenko, S. V. Morozov, H. F. Gleeson, E. W. Hill, A. K. Geim, K. S. Novoselov, *Nano Lett.* **2008**, *8*, 1704.

[10] a) J. T. Robinson, F. K. Perkins, E. S. Snow, Z. Wei, P. E. Sheehan, *Nano Lett.* **2008**, *8*, 3137; b) C. Shan, H. Yang, J. Song, D. Han, A. Ivaska, L. Niu, *Anal. Chem.* **2009**, *81*, 2378

[11] G. Eda, Y. Y. Lin, S. Miller, C. W. Chen, W. F. Su, M. Chhowalla, *Appl. Phys. Lett.* **2008**, *92* (23), 233305.

[12] O. C. Compton, B. Jain, D. A. Dikin, A. Abouimrane, K. Amine, S. T. Nguyen, *Acs Nano* **2011**, *5*, 4380.

[13] a) S. Stankovich, D. A. Dikin, R. D. Piner, K. A. Kohlhaas, A. Kleinhammes, Y. Jia, Y. Wu, S. T. Nguyen, R. S. Ruoff, *Carbon* **2007**, *45*, 1558; b) A. Bagri, C. Mattevi, M. Acik, Y. J. Chabal, M. Chhowalla, V. B. Shenoy, *Nature. Chem.* **2010**, *2*, 581.

[14] a) K. P. Loh, Q. Bao, G. Eda and M. Chhowalla, *Nature. Chem.* **2010**, *2*, 1015; b) D. He, Y. Jiang, H. Lv, M. Pan, S. Mu, *Appl. Cata. B: Envir.* **2013**, *132*, 379.

[15] P. Hongdan, M. Lingjie, L. Qinghua, D. Sheng, F. Zhaofu , J. D. Paul, *J. Mater. Chem.* **2012**, *22*, 14868.

[16] M. Hui-Ling, Z. Hao-Bin, H. Qi-Hui, L. Wen-Juan, J. Zhi-Guo, Y. Zhong-Zhen, D. Aravind, *ACS Appl. Mater.* **2012**, *4*, 1948.

[17] a) M. Alvaro, P. Atienzar, P. de la Cruz, J. L. Delgado, V. Troiani, H. Garcia, F. Langa, A. Palkar, L. Echegoyen, *J. Am. Chem. Soc.* **2006**, *128*, 6626; b) F. Cheng and A. Adronov, *Chem. Mater.* **2006**, *18*, 5389; c) S. Campidelli, C. Sooambar, E. Lozano Diz, C. Ehli, D. M. Guldi, M. Prato, *J. Am. Chem. Soc.* **2006**, *128*, 12544.

[18] a) G. Pagona, A. S. D. Sandanayaka, Y. Araki, J. Fan, N. Tagmatarchis, G. Charalambidis, A. G. Coutsolelos, B. Boitrel, M. Yudasaka, S. Iijima, O. Ito, *Adv. Funct. Mater.* **2007**, *17*, 1705; b) C. Cioffi, S. Campidelli, C. Sooambar, M. Marcaccio, G. Marcolongo, M. Meneghetti, D. Paolucci, F. Paolucci, C. Ehli, G. M. A. Rahman, V. Sgobba, D. M. Guldi, M. Prato, *J. Am. Chem. Soc.* **2007**, *129*, 3938.

[19] a) D. M. Guldi, *Phys. Chem.* **2007**, *9*, 1400; b) V. Sgobba, D. M. Guldi, *J. Mater. Chem.*, 2008, **18**, 153; (c) V. Sgobba, D. M. Guldi, *Chem. Soc. Rev.* **2009**, *38*, 165.

[20] W. S. Hummers, R. E. Offeman, *J. Am. Chem. Soc.* **1958**, *80*, 1339.

[21] L. J. Twyman, J. K. M. Sanders, *Tet. Lett.* **1999**, *40*, 6681.

[22] A. W. Johnson, L. T. Kay, E. Markham, IL Price, I. C. B. Shaw, *J. Chem. Soc.* **1959**, 3416.

[23] H. L. Anderson, J. K. M. Sanders, *J. Chem. Soc., Perkin Trans.1* **1995**, 2223.

[24] W. B. Austin, N. Bilow, W.J. Kelleghan, I. C. S. Y. Lau, *J. Org. Chem.* **1981**, *46*, 2280.

[25] a) C. Gomez-Navarro, R. T. Weitz, A. M. Bittner, M. Scolari, A. Mews, M. Burghard, K. Kern, *Nano Lett.* **2007**, *7*, 3499; b) H. A. Becerril, J. Mao, Z. Liu, R. M. Stoltenberg, Z. Bao, Y. Chen, *ACS Nano*, **2008**, *2*, 463.

[26] M. S. Dresselhaus, A. Jorio, M. Hofmann, G. Dresselhaus, R. Saito, *Nano Lett.* **2010**, *10*, 751.

[27] C. G. Salzmann, B. T. T. Chu, G. Tobias, S. A. Llewellyn, M. L. H. Green, *Carbon* **2007**, *45*, 907.

[28] L. Ballester, A. M. Gil, A. Gutierrez, M. F. Perpinan, M. T. Azcondo, A. E. Sanchez, E. Coronado, C. J. Gomez-Garcia, *Inorg. Chem.* **2000**, *39*, 2837.

[29] A. Das, B. Chakraborty, A. K. Sood, Bull. *Mater. Sci.* **2008**, *31*, 579.

[30] M.B. Krishan, N. Venkatramaiah, R, Vankatesan and D.N.Rao, *J. Mater. Chem.* **2012**, *22*, 3059.

[31] E. W. Meijer, *Chem Rev* **2009**, *109*, 5687.

[32] J. K. Sprafke, S. D. Stranks, J. H. Warner, R. J. Nicholas, H. L. Anderson, *Angew. Chem. Int. Ed.* **2011**, *50*, 2313.

[33] a) A. L. Kieran, A. D. Bond, A. M. Belenguer, *Chem. Com.* **2003**, *21*, 2674; b) C. C. Mak, N. Bampos, J. K. Sanders, *Angew. Chem. Int. Ed.* **1998**, *37*, 3020.

[34] A. Altomare, G. Carascano, C. Giacovazzo, A. Guagliardi, *J. Appl. Crystallogr.* **1993**, *26*, 343.

[35] D. J. Watkin, C. K. Prout, J. R. Carruthers, P. W. Betteridge, *CRYSTALS*, Oxford, UK, 1996.

[36] P. W. Betteridge, J. R. Carruthers, R. I. Cooper, K. Prout, D. J. Watkin, *J. Appl. Crystallogr.* **2003**, *36*, 1487.

[37] D. J. Watkin, C. K. Prout, L. J. Pearce, *CAMERON*, Oxford, UK, 1996.

[38] N. Walker, D. Stuart, *Acta Crystallogr., Sect. A* **1983**, *39*, 158.

Design and synthesis of a novel porphyrin-based nanohybrid, whereby the entire surface of GO is modified via supramolecular assembly. The resulting Zn(II)-porphyrin@GO nanohybrid forms stable dispersions in ethanol. The established synthetic methodology presented here is of great interest due to open new opportunities in the use of uniform dispersions of tailed nanohybrid GO layered materials.

Porphyrin, graphene oxide, AFM studies, UV-vis titrations, fluorescence titrations

B. Mao, D. G. Calatayud, V. Mirabello, Benjamin J. Hodges, J. A. Martins, S. W. Botchway, J. Mitchels and Sofia I. Pascu*

Interactions Between an Aryl Thioacetate-Functionalised Zn(II) Porphyrin and Graphene Oxide

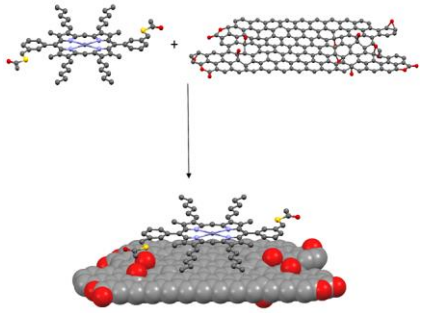

ToC figure